

# The NIST compilation of ionization potentials revisited: From He-like to Xe-like ions

Gabriel Gil and Augusto González

*Instituto de Cibernética, Matemática y Física, Calle E 309, Vedado, La Habana, Cuba*

The National Institute of Standards and Technology (NIST) database on ionization potentials for neutral atoms and ions is examined. For each isoelectronic sequence, we construct a regularized perturbative series that exactly matches the large- $Z$  and  $Z \approx N - 1$  regions. Comparison of the NIST data with this series allows the identification of problematic data values.

PACS numbers: 32.30.-r, 32.10.Hq, 31.15.-p

Physics is indeed a mature science. Large amounts of data, of very different kinds, have been accumulated along decades. Sometimes, a fresh look at these compilations, on the basis of simple -physically meaningful- models, leads to a qualitative understanding of the data.

In a previous paper<sup>1</sup>, we show that the NIST data on ionization potentials of atomic ions<sup>2</sup> can be accomodated along a single universal curve, based on Thomas-Fermi scaling features.

In the present work, we go a step further and develop a simple model allowing the identification of problematic isolated reported values in a particular isoelectronic sequence. Because of the fact that the compilation is very often used for different purposes, indications of which data could be wrong and should be re-examined is of great importance. For instance, as commented in Ref. [3], accurate description of the spectra is useful in order to model some dynamical features of stellar sources, and also to interpret astronomical data.

Our model for the ionization potential is a smooth interpolation that matches both the large- $Z$  (heavy ion) and the  $Z \approx N - 1$  (anion) regions.<sup>4</sup> We call it the “regularized perturbation theory” (RPT). We have used similar approaches in order to compute the energy of relatively large quantum dots,<sup>5</sup> atomic ions in a harmonic trap,<sup>6</sup> neutral atoms in traps,<sup>7</sup> and Rydberg-like impurity levels in a quantum well.<sup>8</sup>

The RPT series for the ionization potential of an  $N$ -electron atomic ion with nuclear charge  $Z$  is written as (atomic units are used everywhere):<sup>4,9</sup>

$$I_p = a_2 Z^2 + a_1 Z + a_0 + a_{-1}/Z. \quad (1)$$

Coefficients  $a_2$  and  $a_1$  are obtained from the large- $Z$  limit.<sup>4</sup>  $a_2$  comes from the leading term (free electrons in the nuclear field), whereas  $a_1$  is computed in the next-to-leading approximation, where Coulomb repulsion between electrons is perturbatively treated. Relativistic corrections should be included because the NIST data span the range of nuclear charges up to very heavy ions, i.e.  $N \leq Z \leq 110$ . Detailed expressions for  $a_2$  and  $a_1$ , with explicit relativistic corrections, can be found in Ref. [4].

The next two terms of the series have the functional form suggested by higher-order perturbation theory on the Coulomb repulsion. However, in order to determine

them, we shall follow a different strategy. We force expression (1) to match the expected value and the slope at  $Z = N - 1$ .<sup>4</sup> In this sense, it is a “regularized perturbative series”. These conditions are written as follows:

$$I_p|_{Z=N-1} = E_a(N - 1), \\ \left. \frac{dI_p}{dZ} \right|_{Z=N-1} = s = \frac{\int_R^\infty dr e^{2\kappa r}/r}{\int_R^\infty dr e^{2\kappa r}}. \quad (2)$$

$E_a(N - 1)$  is the electron affinity of the neutral atom with  $N - 1$  electrons.<sup>10</sup> The slope  $s$ , on the other hand, is computed in terms of  $E_a(N - 1)$  and  $R(N - 1)$ , that is a characteristic radius of the  $(N - 1)$ -electron system which we estimate as the covalent radius.<sup>9</sup> Note that  $\kappa = \sqrt{2E_a}$ . The expression of the slope makes use of the fact that, at  $Z = N - 1$ , the outer electron interacts with a neutral core. Thus, the interaction is short-ranged and the wave function at large distances is solely determined by the binding energy, i.e.  $E_a(N - 1)$ . We use this function in order to perturbatively compute the residual Coulomb interaction of the outer electron with the core, when  $Z$  is slightly displaced from  $N - 1$ . The explicit expression for  $s$  was derived earlier in Ref. [9].

Once the coefficients in Eq. 1 are determined, our RPT series provides an interpolation for intermediate values of  $Z$ . We show in Fig. 1, in quality of example, the series for Ne-like ions ( $N = 10$ ) along with the corresponding NIST data.

Some comments should be added to this figure. First, the dependence of  $I_p$  on  $Z$  is smooth. It is difficult to distinguish a problematic point, even if we change the scale. Second, generally NIST reported values are experimental data only when  $Z$  is close to  $N$ . For larger  $Z$ , data come from calculations or interpolations. Thus, we expect relatively high errors in this regime. Relative deviations of the RPT from NIST data are only a few percents in the intermediate- $Z$  region, which is a common feature of interpolants.<sup>5,6,7,8</sup>

Notice that the difference  $|RPT - NIST|$  allows us to identify problematic points, as they apparently deviate from the neighboring points. In the appendices, we examine 42 isoelectronic sequences (five rows of the Mendeleev Table), from He-like to Xe-like ions. In this range, only the atoms which do not have an stable singly charged anion are excluded.

The remarkable deviations at  $Z = 74$ ,<sup>11</sup> and the abrupt jump at  $Z \approx 51$ ,<sup>12</sup> just to mention a few examples common to many of the isoelectronic sequences, are clear indications of deficiencies in the computed data reported by NIST. The dispersion of the data for very heavy ions should also motivate a reconsideration of the Dirac-Fock calculations.<sup>12</sup>

We hope that the present analysis will be helpful in order to improve the reference data.

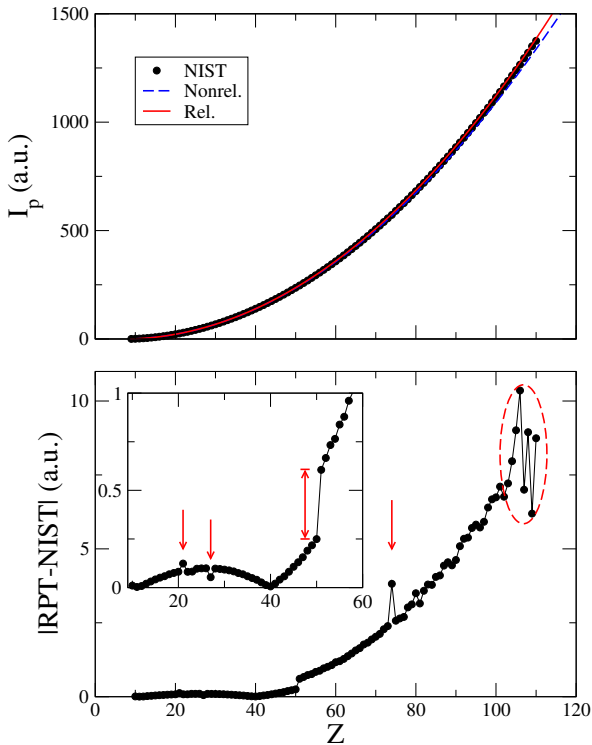


FIG. 1. (Color online) Ne-like ions ( $N = 10$ ). Upper panel: Ionization potentials taken from the NIST compilation along with our nonrelativistic (discontinuous, blue) and relativistically corrected (continuous, red) RPT predictions versus atomic number. Curves are smooth at any scale. Lower panel: Absolute value of the difference between the relativistic RPT series and the NIST reported values versus atomic number. Detected inconsistencies ( $Z = 21, 27, 74$  and the abrupt jump at  $Z \approx 51$ ) are marked with red arrows. We point out also the great dispersion of the data for  $Z \geq 102$  (discontinuous red ellipse).

#### Appendix A: The He-like sequence ( $N = 2$ )

RPT coefficients:

$$\begin{aligned} a_2 &= 0.5 + 0.125 (Z/137.0)^2, \\ a_1 &= -0.625 - 0.0989536 (Z/137.0)^2, \\ a_0 &= 0.368987, \\ a_{-1} &= -0.216282. \end{aligned}$$

Conditions at  $Z = N - 1$ :

$$\begin{aligned} E_a(\text{H}) &= 0.0277063, \\ s &= 0.59129. \end{aligned} \quad (\text{A1})$$

The slope was computed from  $E_a(\text{H})$  and  $R_{\text{cov}}(\text{H}) = 0.604712$ . Here, and in the analysis below, data for  $E_a$  and  $R_{\text{cov}}$  are taken from Ref. 10.

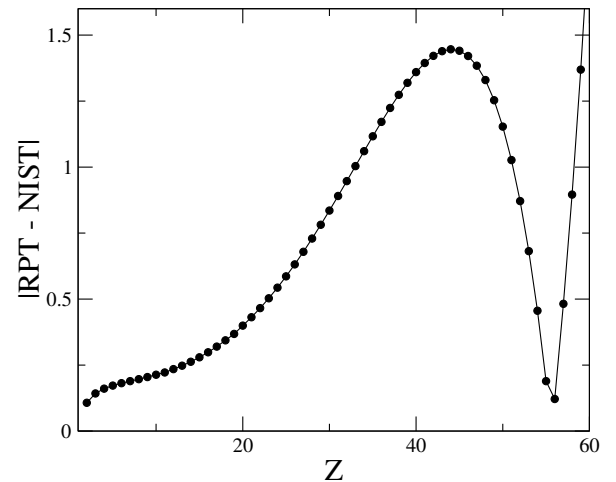


FIG. 2. (Color online) The He-like systems ( $N = 2$ ). Absolute value of the difference between the relativistic RPT and the NIST values versus atomic number. No inconsistencies were detected.

#### Discussion:

Let us comment on some features of the He-like case. In the range  $2 \leq Z \leq 60$ , the difference between our RPT series and the reported values is very well behaved. It is exactly zero in the anionic region and tends to low values at  $Z \approx 55$ . In the intermediate region, the maximum relative error is around 0.15%.

When  $Z \geq 56$ ,  $| \text{RPT-NIST} |$  rises again. NIST ionization potentials in the  $12 \leq Z \leq 100$  range come mainly from *ab initio* QED calculations by Artemyev *et al.*,<sup>13</sup> which include finite nuclear-size effects. It is natural that our perturbative treatment of relativity cannot reproduce their results for very large  $Z$ .

#### Appendix B: Second row elements

##### 1. The Be-like sequence ( $N = 4$ )

RPT coefficients:

$$\begin{aligned} a_2 &= 0.125 + 0.0390625 (Z/137.0)^2, \\ a_1 &= -0.548196 - 0.0952831 (Z/137.0)^2, \\ a_0 &= 0.675679, \\ a_{-1} &= -0.400253. \end{aligned}$$

Conditions at  $Z = N - 1$ :

$$E_a(\text{Li}) = 0.0227050, \\ s = 0.246343. \quad (\text{B1})$$

The slope was computed from  $E_a(\text{Li})$  and  $R_{cov}(\text{Li}) = 2.456644$ .

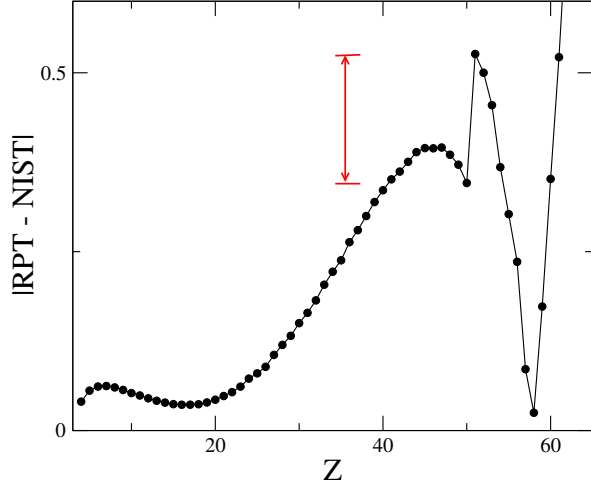


FIG. 3. (Color online) The Be-like isoelectronic sequence ( $N = 4$ ). Detected inconsistency (an abrupt jump at  $Z \approx 51$ ) is marked with red arrows.

### Discussion:

The comparison between NIST and RPT values for the Be-like sequence shows an abrupt jump of 0.28 a.u. at  $Z \approx 51$  (see Fig. 3). These are numbers based on Dirac-Fock calculations of  $I_p$  computed by different groups. When  $Z \leq 51$ , numbers come from Ref. [14], whereas for  $Z > 51$  almost all reported numbers come from Rodrigues *et al.*<sup>12</sup>. We notice that, in Ref. [14], a formula like Eq. (1) is used as a fit to correct the computed values.

In spite of the fact that our RPT series lacks of spectroscopic precision, every jump or deviation in  $|\text{RPT}-\text{NIST}|$  can be taken as a signature of possible errors.

### 2. The C-like sequence ( $N = 6$ )

RPT coefficients:

$$a_2 = 0.125 + 0.0390625 (Z/137.0)^2, \\ a_1 = -0.945089 - 0.241928 (Z/137.0)^2, \\ a_0 = 0.0390625, \\ a_{-1} = 0.643271.$$

Conditions at  $Z = N - 1$ :

$$E_a(\text{B}) = 0.0102761, \\ s = 0.279379. \quad (\text{B2})$$

The slope was computed from  $E_a(\text{B})$  and  $R_{cov}(\text{B}) = 1.58737$ .

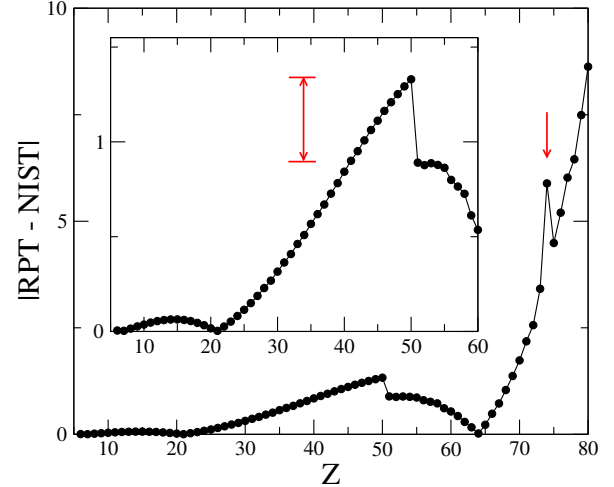


FIG. 4. (Color online) The C-like systems ( $N = 6$ ). Detected inconsistencies ( $Z = 74$  and an abrupt jump at  $Z \approx 51$ ) are marked with red arrows.

### Discussion:

Analysis of Fig. 4 (C-like sequence) also shows an abrupt jump of nearly 0.43 a.u. at  $Z \approx 51$ . As in the He-like case, this jump is associated to changes in the calculation methodology.

In addition, an apparent deviation in the ionization potential appears at  $Z = 74$ . This number, corresponding to a tungsten heavy ion ( $\text{W}^{+68}$ ), was collected by NIST compilers Kramida and Reader with the help of a semi-empirical approach<sup>11</sup>.

### 3. The N-like sequence ( $N = 7$ )

RPT coefficients:

$$a_2 = 0.125 + 0.0078125 (Z/137.0)^2, \\ a_1 = -1.10915 - 0.152346 (Z/137.0)^2, \\ a_0 = 2.26192, \\ a_{-1} = -0.356612.$$

Conditions at  $Z = N - 1$ :

$$E_a(\text{C}) = 0.0463657, \\ s = 0.400642. \quad (\text{B3})$$

The slope was computed from  $E_a(\text{C})$  and  $R_{cov}(\text{C}) = 1.417295$ .

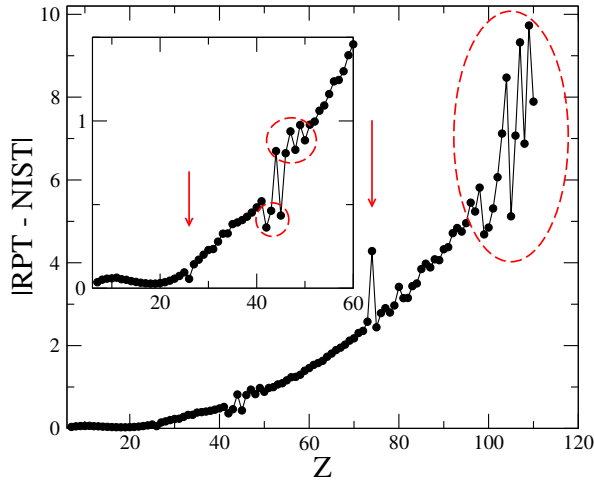


FIG. 5. (Color online) The N-like ions ( $N = 7$ ). Detected inconsistencies ( $Z = 26$ ,  $Z = 42-50$ ,  $Z = 74$  and the great dispersion for  $Z \geq 96$ ) are marked with red arrows and discontinuous red ellipses.

### Discussion:

The N-like sequence (Fig. 5) presents remarkable inconsistencies at  $Z = 26$ ,  $42-50$  and, once more, at  $Z = 74$ . The ionization potential for  $Z = 26$  was taken from the paper by Sugar and Corliss.<sup>15</sup> Points for  $Z = 42-50$  come from the Dirac-Fock calculations by Biémont *et al.*<sup>14</sup> The reported large uncertainty of 1.5 a.u. is consistent with the deviations. The  $Z = 74$  case, again taken from Ref. [11], shows a deviation of approximately 2 a.u. from the average curve. Besides, the great dispersion for  $Z \geq 96$ , questions the consistency of Dirac-Fock calculations by Rodrigues *et al.*<sup>12</sup> for highly charged ions. Notice, however, that most deviations are within error bars, which are remarkably high (from 1.5 to 20 a.u.) for  $Z \geq 73$ .

### 4. The F-like sequence ( $N = 9$ )

RPT coefficients:

$$\begin{aligned} a_2 &= 0.125 + 0.0078125 (Z/137.0)^2, \\ a_1 &= -1.4654 - 0.181681 (Z/137.0)^2, \\ a_0 &= 2.79034, \\ a_{-1} &= 7.91836. \end{aligned}$$

Conditions at  $Z = N - 1$ :

$$\begin{aligned} E_a(O) &= 0.0536759, \\ s &= 0.410681. \end{aligned} \quad (B4)$$

The slope was computed from  $E_a(O)$  and  $R_{cov}(O) = 1.417295$ .

### Discussion:

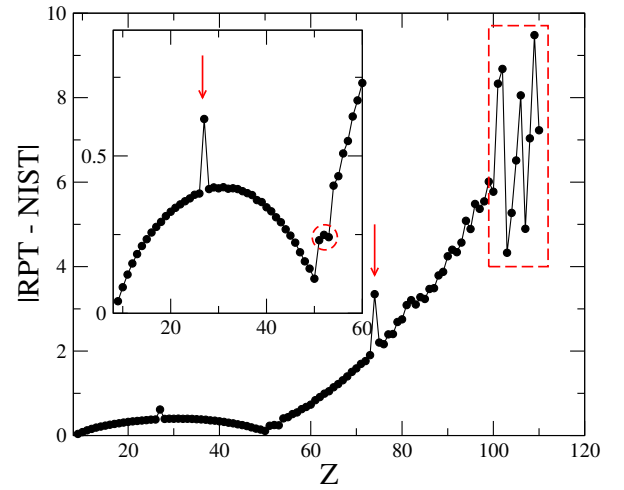


FIG. 6. (Color online) The F-like sequence ( $N = 9$ ). Detected inconsistencies ( $Z = 27$ ,  $51-53$ ,  $74$ , and the great dispersion for  $Z > 100$ ) are marked with red arrows and discontinuous red ellipses and box.

In the F-like sequence (Fig. 6), great deviations are noticed for  $Z = 27$  and  $74$ .  $I_p$  for  $Z = 27$  comes from Ref. [15], the very same paper by Sugar and Corliss cited in the N-like case.  $Z = 74$  belongs to the case of tungsten ions ( $W^{+65}$ ) and the  $I_p$  value is, once more, taken from Ref. [11]. Other inconsistencies detected are the group of points in  $Z = 51 - 53$ ,<sup>12</sup> and the great dispersion of the data for  $Z > 100$ , the latter coming again from the Dirac-Fock calculations of Ref. [12]. It is also worth mentioning the large error bars reported for  $Z \geq 75$ .

### 5. The Ne-like sequence ( $N = 10$ )

RPT coefficients:

$$\begin{aligned} a_2 &= 0.125 + 0.0078125 (Z/137.0)^2, \\ a_1 &= -1.63649 - 0.195621 (Z/137.0)^2, \\ a_0 &= 4.13824, \\ a_{-1} &= 5.3556. \end{aligned}$$

Conditions at  $Z = N - 1$ :

$$\begin{aligned} E_a(F) &= 0.124985, \\ s &= 0.547149. \end{aligned} \quad (B5)$$

The slope was computed from  $E_a(F)$  and  $R_{cov}(F) = 1.13384$ .

### Discussion:

In the Ne-like sequence (Fig. 1), deviations at  $Z = 21$  and  $Z = 27$  are related to Ref. [15]. The  $Z = 74$  case,<sup>11</sup> is found again as a clear inconsistent one. Other inconsistencies detected are the previously discussed abrupt jump at  $Z \approx 51$  and the great dispersion for  $Z \geq 101$ , related to Dirac-Fock calculations<sup>12</sup>. For  $Z \geq 76$  deviations are within uncertainty bars.

## Appendix C: Third row elements

### 1. The Mg-like sequence ( $N = 12$ )

RPT coefficients:

$$\begin{aligned} a_2 &= 0.0555556 + 0.0138889 (Z/137.0)^2, \\ a_1 &= -0.931477 - 0.0906944 (Z/137.0)^2, \\ a_0 &= 2.62996, \\ a_{-1} &= 10.0077. \end{aligned}$$

Conditions at  $Z = N - 1$ :

$$\begin{aligned} E_a(\text{Na}) &= 0.0201287, \\ s &= 0.209421. \end{aligned} \quad (\text{C1})$$

The slope was computed from  $E_a(\text{Na})$  and  $R_{cov}(\text{Na}) = 3.023562$ .

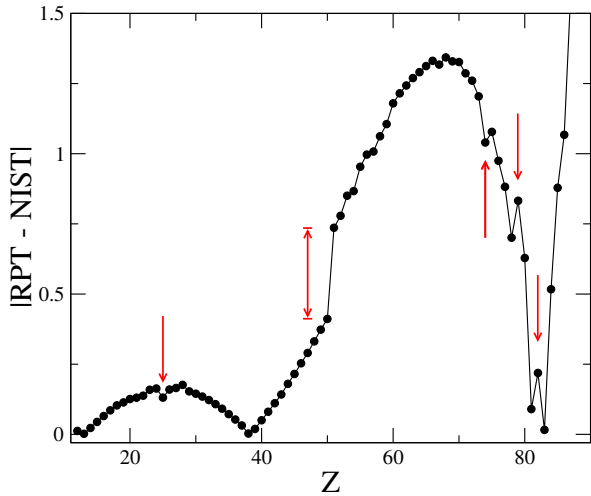


FIG. 7. (Color online) Mg-like systems ( $N = 12$ ). Detected inconsistencies ( $Z = 25$ , the jump at  $Z \approx 51$ ,  $Z = 74, 79$  and  $82$ ) are marked with red arrows.

### Discussion:

Mg-like sequence (Fig. 7) of ions shows a clear deviation at  $Z = 25$ , related to Ref. 15. The jump at  $Z \approx 51$  and the deviation at  $Z = 74$  were discussed above. We may stress that the magnitude of the jump diminishes with  $N$ . In addition, we observe deviations at  $Z = 79$  and  $83$ , data coming from Rodrigues calculations<sup>12</sup>. Notice that many of these problematic cases are apparent in many sequences. Below, we will discuss only new events.

### 2. The Si-like sequence ( $N = 14$ )

RPT coefficients:

$$a_2 = 0.0555556 + 0.0138889 (Z/137.0)^2,$$

$$\begin{aligned} a_1 &= -1.13489 - 0.148767 (Z/137.0)^2, \\ a_0 &= 4.44303, \\ a_{-1} &= 12.1396. \end{aligned}$$

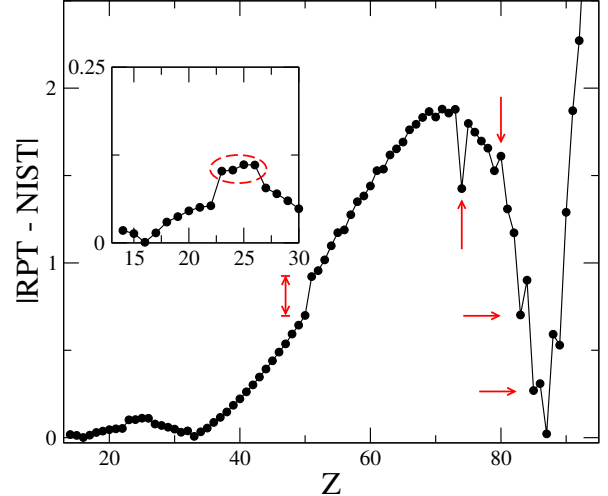


FIG. 8. (Color online) The Si-like sequence ( $N = 14$ ). Detected inconsistencies (the group of points around  $Z = 25$ , the jump at  $Z \approx 51$ ,  $Z = 74, 80, 83$  and  $85$  are marked with red arrows and ellipse).

Conditions at  $Z = N - 1$ :

$$\begin{aligned} E_a(\text{Al}) &= 0.0159006, \\ s &= 0.239636. \end{aligned} \quad (\text{C2})$$

The slope was computed from  $E_a(\text{Al})$  and  $R_{cov}(\text{Al}) = 2.343260$ .

### 3. The P-like sequence ( $N = 15$ )

RPT coefficients:

$$\begin{aligned} a_2 &= 0.0555556 + 0.00462963 (Z/137.0)^2, \\ a_1 &= -1.19956 - 0.109484 (Z/137.0)^2, \\ a_0 &= 5.24386, \\ a_{-1} &= 10.0615. \end{aligned}$$

Conditions at  $Z = N - 1$ :

$$\begin{aligned} E_a(\text{Si}) &= 0.0510817, \\ s &= 0.304873. \end{aligned} \quad (\text{C3})$$

The slope was computed from  $E_a(\text{Si})$  and  $R_{cov}(\text{Si}) = 2.154288$ .

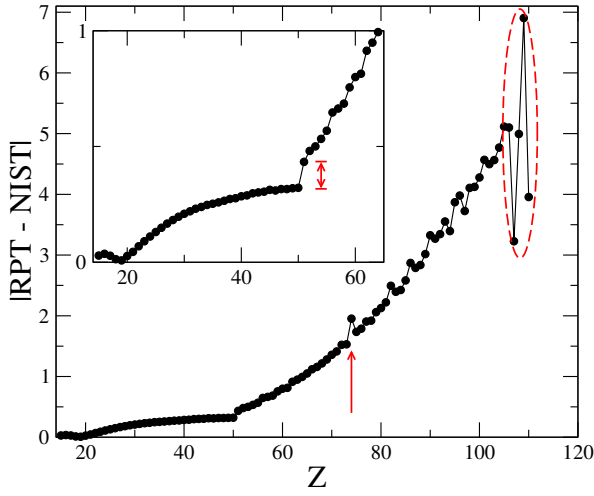


FIG. 9. (Color online) The P-like systems ( $N = 15$ ). Detected inconsistencies (the jump at  $Z \approx 51$ ,  $Z = 74$ , and a great dispersion for  $Z \geq 106$ ) are marked with red arrows and a discontinuous red ellipse. Notice that the dispersion in fact begins for  $Z \geq 82$ , although for very large values of  $Z$  becomes more significant.

#### 4. The S-like sequence ( $N = 16$ )

RPT coefficients:

$$\begin{aligned} a_2 &= 0.0555556 + 0.00462963 (Z/137.0)^2, \\ a_1 &= -1.26711 - 0.114919 (Z/137.0)^2, \\ a_0 &= 4.83765, \\ a_{-1} &= 25.569. \end{aligned}$$

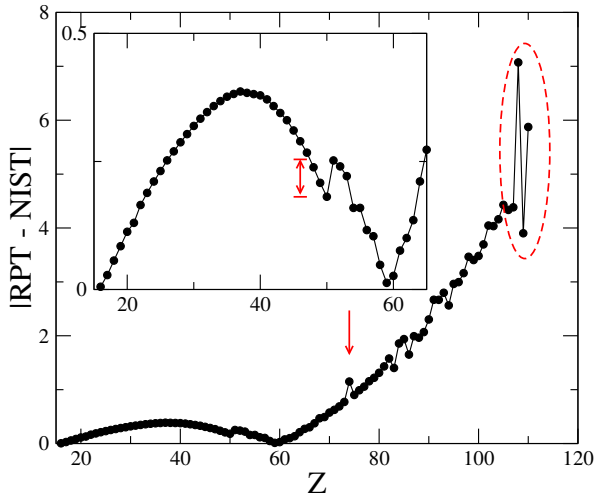


FIG. 10. (Color online) The S-like ions ( $N = 16$ ). Detected inconsistencies (the jump at  $Z \approx 51$ ,  $Z = 74$ , and a great dispersion for  $Z \geq 106$ ) are marked with red arrows and a discontinuous red ellipse. Notice, once more, that the dispersion in fact begins for  $Z \geq 83$ .

Conditions at  $Z = N - 1$ :

$$\begin{aligned} E_a(P) &= 0.0274519, \\ s &= 0.286207. \end{aligned} \quad (C4)$$

The slope was computed from  $E_a(P)$  and  $R_{cov}(P) = 2.0598015$ .

#### 5. The Cl-like sequence ( $N = 17$ )

RPT coefficients:

$$\begin{aligned} a_2 &= 0.0555556 + 0.00462963 (Z/137.0)^2, \\ a_1 &= -1.34042 - 0.121136 (Z/137.0)^2, \\ a_0 &= 5.81594, \\ a_{-1} &= 23.9212. \end{aligned}$$

Conditions at  $Z = N - 1$ :

$$\begin{aligned} E_a(S) &= 0.0763283, \\ s &= 0.344289. \end{aligned} \quad (C5)$$

The slope was computed from  $E_a(S)$  and  $R_{cov}(S) = 1.965315$ .

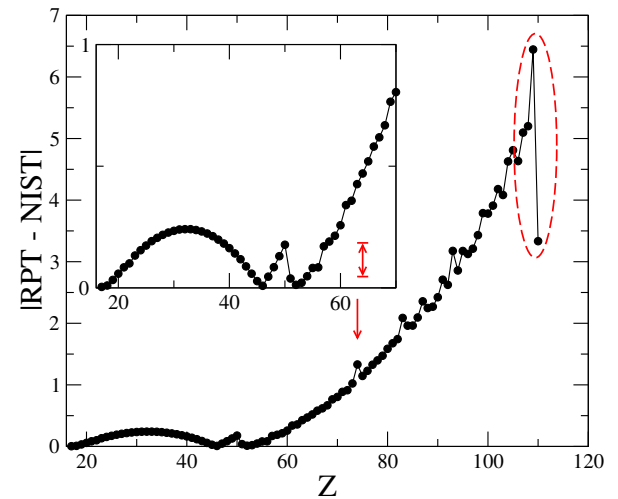


FIG. 11. (Color online) Cl-like systems ( $N = 17$ ). Detected inconsistencies (the jump at  $Z \approx 51$ ,  $Z = 74$ , and a great dispersion for  $Z \geq 106$ ) are marked with red arrows and a discontinuous red ellipse.

#### 6. The Ar-like sequence ( $N = 18$ )

RPT coefficients:

$$\begin{aligned} a_2 &= 0.0555556 + 0.00462963 (Z/137.0)^2, \\ a_1 &= -1.40796 - 0.12657 (Z/137.0)^2, \\ a_0 &= 6.30212, \\ a_{-1} &= 29.2914. \end{aligned}$$

Conditions at  $Z = N - 1$ :

$$E_a(\text{Cl}) = 0.132775, \\ s = 0.380045. \quad (\text{C6})$$

The slope was computed from  $E_a(\text{Cl})$  and  $R_{\text{cov}}(\text{Cl}) = 1.889726$ .

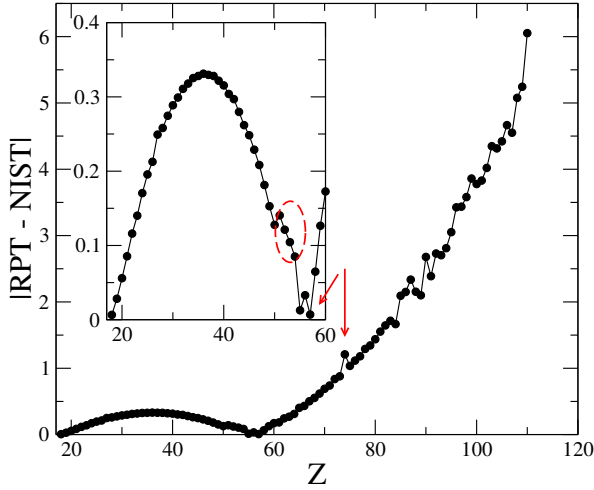


FIG. 12. (Color online) The Ar-like systems ( $N = 18$ ). In this case, we distinguish the group of points in  $51 \leq Z \leq 54$ ,<sup>12</sup> and the deviations at  $Z = 57$ <sup>12</sup> and  $74$ .<sup>11</sup> Dispersion of points for  $Z \geq 83$  is noticeable, but was not marked.

#### Appendix D: Four row elements

##### 1. The Ca-like sequence ( $N = 20$ )

RPT coefficients:

$$a_2 = 0.0555556 + 0.00462963 (Z/137.0)^2, \\ a_1 = -1.70312 - 0.200236 (Z/137.0)^2, \\ a_0 = 7.96996, \\ a_{-1} = 83.4702.$$

Conditions at  $Z = N - 1$ :

$$E_a(\text{K}) = 0.0184220, \\ s = 0.176307. \quad (\text{D1})$$

The slope was computed from  $E_a(\text{K})$  and  $R_{\text{cov}}(\text{K}) = 3.779452$ .

##### Discussion:

The Ca-like sequence is the first with a rearrangement of the electronic spectrum with the increase of  $Z$ . For  $Z \approx N$  the last two electrons occupy the 4s subshell, whereas for larger  $Z$  they move to the 3d orbital. The

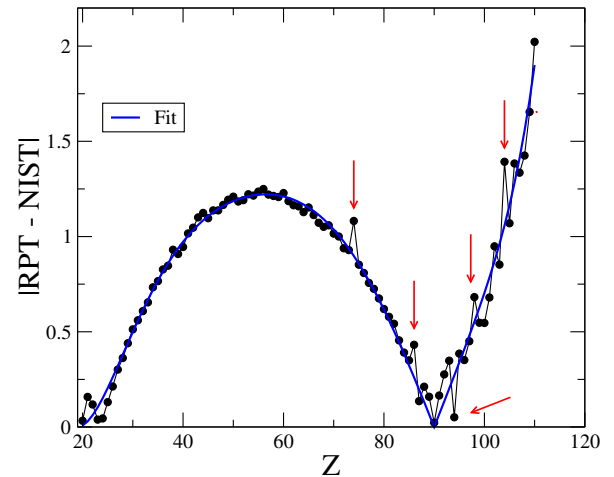


FIG. 13. (Color online) The Ca-like systems ( $N = 20$ ). Detected inconsistencies ( $Z = 74, 86, 94, 98$  and  $104$ ) are marked with red arrows. They are easily detected when compared with the average curve, Eq. (D2).

observed peak at  $Z = 21 - 22$  is surely related to this fact.

For  $Z \geq 86$  there are a relatively large dispersion of data and a crossing point of the NIST and RPT curves. In order to distinguish problematic points, we find most convenient to draw the average curve with the help of the following model:

$$|\text{NIST} - \text{RPT}|_{av} = (Z - N + 1)^2 \left[ \prod_i (Z - Z_i) \right] \times \\ (a_0 + a_1 Z + a_2 Z^2 + a_3 Z^3 + a_4 Z^4). \quad (\text{D2})$$

The first factor is due to the fact that at  $Z = N - 1$  we fit the value and the derivative of  $I_p$ .  $Z_i$  are crossing points (only one for Ca), and  $a_j$  are fitting parameters. This average model will be useful in other situations below.

##### 2. The Sc-like sequence ( $N = 21$ )

RPT coefficients:

$$a_2 = 0.0555556 + 0.00462963 (Z/137.0)^2, \\ a_1 = -1.79098 - 0.209669 (Z/137.0)^2, \\ a_0 = 7.18837, \\ a_{-1} = 129.196.$$

Conditions at  $Z = N - 1$ :

$$E_a(\text{Ca}) = 0.000901924, \\ s = 0.107729. \quad (\text{D3})$$

The slope was computed from  $E_a(\text{Ca})$  and  $R_{\text{cov}}(\text{Ca}) = 3.288123$ .

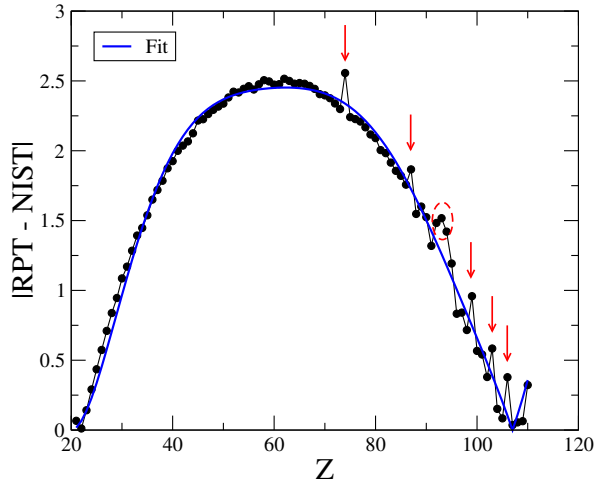


FIG. 14. (Color online) The Sc-like systems ( $N = 21$ ). Detected inconsistencies ( $Z = 74, 87, 92-94, 99, 103$  and  $106$ ) are marked with red arrows.

### 3. The Ti-like sequence ( $N = 22$ )

RPT coefficients:

$$\begin{aligned} a_2 &= 0.0555556 + 0.00462963 (Z/137.0)^2, \\ a_1 &= -1.87158 - 0.218161 (Z/137.0)^2, \\ a_0 &= 8.87906, \\ a_{-1} &= 125.803. \end{aligned}$$

Conditions at  $Z = N - 1$ :

$$\begin{aligned} E_a(\text{Sc}) &= 0.00690650, \\ s &= 0.175933. \end{aligned} \quad (\text{D4})$$

The slope was computed from  $E_a(\text{Sc})$  and  $R_{cov}(\text{Sc}) = 3.004665$ .

### 4. The V-like sequence ( $N = 23$ )

RPT coefficients:

$$\begin{aligned} a_2 &= 0.0555556 + 0.00462963 (Z/137.0)^2, \\ a_1 &= -1.95847 - 0.154589 (Z/137.0)^2, \\ a_0 &= 8.95387, \\ a_{-1} &= 160.08. \end{aligned}$$

Conditions at  $Z = N - 1$ :

$$\begin{aligned} E_a(\text{Ti}) &= 0.00290230, \\ s &= 0.156499. \end{aligned} \quad (\text{D5})$$

The slope was computed from  $E_a(\text{Ti})$  and  $R_{cov}(\text{Ti}) = 2.721206$ .

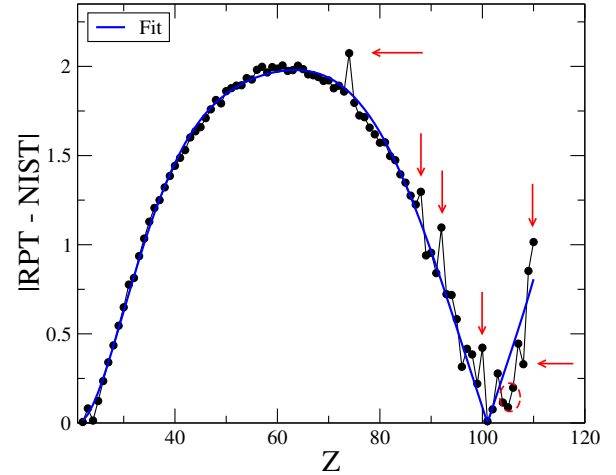


FIG. 15. (Color online) Ti-like systems ( $N = 22$ ). Detected inconsistencies ( $Z = 74, 88, 92, 100, 104-106, 108$  and  $110$ ) are marked with red arrows.

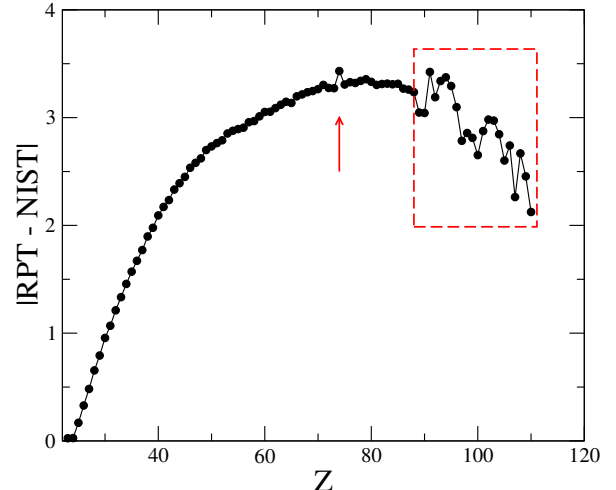


FIG. 16. (Color online) The V-like ions ( $N = 23$ ). Detected inconsistencies ( $Z = 74$  and a great dispersion for  $Z \geq 89$ ) are marked with a red arrow and a discontinuous red box.

### 5. The Cr-like sequence ( $N = 24$ )

RPT coefficients:

$$\begin{aligned} a_2 &= 0.0555556 + 0.00154321 (Z/137.0)^2, \\ a_1 &= -2.03885 - 0.15826 (Z/137.0)^2, \\ a_0 &= 10.9246, \\ a_{-1} &= 153.618. \end{aligned}$$

Conditions at  $Z = N - 1$ :

$$\begin{aligned} E_a(\text{V}) &= 0.0192866, \\ s &= 0.223850. \end{aligned} \quad (\text{D6})$$

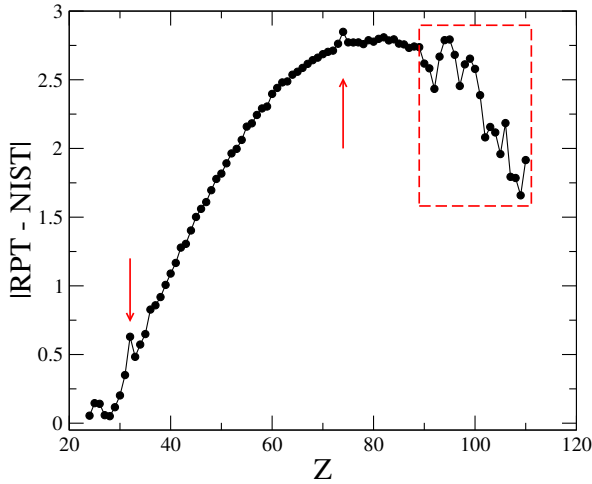


FIG. 17. (Color online) The Cr-like sequence ( $N = 24$ ). Detected inconsistencies ( $Z = 32$ ,  $Z = 74$  and a great dispersion for  $Z \geq 90$ ) are marked with red arrows and a discontinuous red box.

The slope was computed from  $E_a(V)$  and  $R_{cov}(V) = 2.721206$ .

#### Discussion:

In the Cr-like sequence, we shall distinguish the problematic point at  $Z = 32$ , coming from the paper by Sugar and Musgrave<sup>16</sup>. We shall stress also that, for  $Z \geq 90$ , the reported error bars range from 1.5 to 10 a.u.

#### 6. The Mn-like sequence ( $N = 25$ )

RPT coefficients:

$$\begin{aligned} a_2 &= 0.0555556 + 0.00154321 (Z/137.0)^2, \\ a_1 &= -2.12264 - 0.162119 (Z/137.0)^2, \\ a_0 &= 12.0502, \\ a_{-1} &= 168.234. \end{aligned}$$

Conditions at  $Z = N - 1$ :

$$\begin{aligned} E_a(\text{Cr}) &= 0.0244666, \\ s &= 0.249254. \end{aligned} \quad (\text{D7})$$

The slope was computed from  $E_a(\text{Cr})$  and  $R_{cov}(\text{Cr}) = 2.456644$ .

#### 7. The Co-like sequence ( $N = 27$ )

RPT coefficients:

$$\begin{aligned} a_2 &= 0.0555556 + 0.00154321 (Z/137.0)^2, \\ a_1 &= -2.29511 - 0.170117 (Z/137.0)^2, \\ a_0 &= 11.9833, \\ a_{-1} &= 266.793. \end{aligned}$$

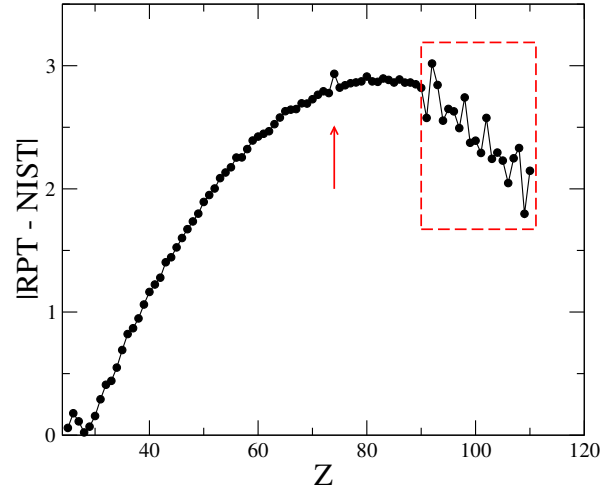


FIG. 18. (Color online) The Mn-like systems ( $N = 25$ ). Detected inconsistencies ( $Z = 74$  and a great dispersion for  $Z \geq 91$ ) are marked with a red arrow and a discontinuous red box.

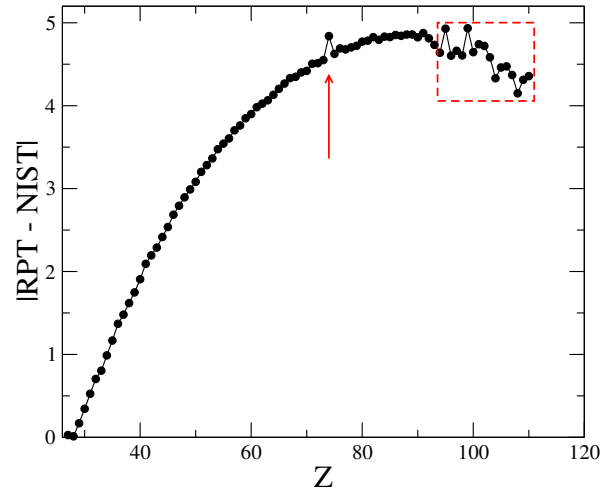


FIG. 19. (Color online) The Co-like sequence ( $N = 27$ ). Detected inconsistencies ( $Z = 74$  and the dispersion of points for  $Z \geq 93$ ) are marked with a red arrow and box. Dispersed points, however, lie within error bars, of around 2 a.u.

Conditions at  $Z = N - 1$ :

$$\begin{aligned} E_a(\text{Fe}) &= 0.00554713, \\ s &= 0.195878. \end{aligned} \quad (\text{D8})$$

The slope was computed from  $E_a(\text{Fe})$  and  $R_{cov}(\text{Fe}) = 2.343260$ .

#### 8. The Ni-like sequence ( $N = 28$ )

RPT coefficients:

$$a_2 = 0.0555556 + 0.00154321 (Z/137.0)^2,$$

$$\begin{aligned} a_1 &= -2.3755 - 0.173789 (Z/137.0)^2, \\ a_0 &= 14.2165, \\ a_{-1} &= 258.787. \end{aligned}$$

Conditions at  $Z = N - 1$ :

$$\begin{aligned} E_a(\text{Co}) &= 0.0243196, \\ s &= 0.266002. \end{aligned} \quad (\text{D9})$$

The slope was computed from  $E_a(\text{Co})$  and  $R_{cov}(\text{Co}) = 2.229877$ .

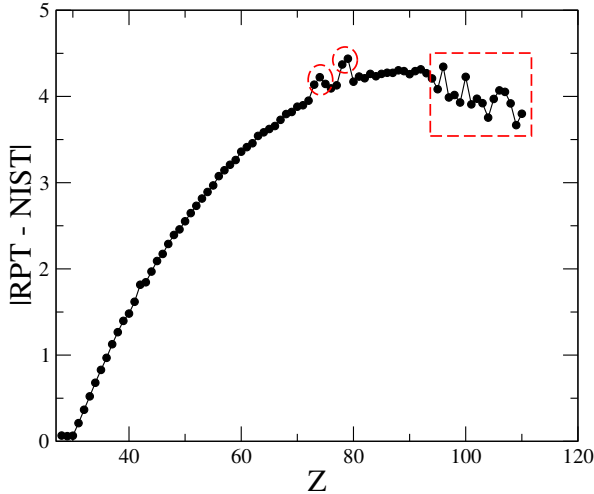


FIG. 20. (Color online) The Ni-like systems ( $N = 28$ ). Detected inconsistencies ( $Z = 73 - 75$ ,  $78 - 79$  and a great dispersion for  $Z \geq 95$ ) are marked with discontinuous red ellipses and box.

#### Discussion:

The Ni-like ions (Fig. 20) shows deviations for  $Z = 73 - 75$  and  $78 - 79$ , both coming from the paper by Tragin *et al.*<sup>17</sup>. In most cases, the error bars are greater than deviations.

#### 9. The Cu-like sequence ( $N = 29$ )

RPT coefficients:

$$\begin{aligned} a_2 &= 0.03125 + 0.00634766 (Z/137.0)^2, \\ a_1 &= -1.34713 - 0.0620302 (Z/137.0)^2, \\ a_0 &= 9.66505, \\ a_{-1} &= 96.9281. \end{aligned}$$

Conditions at  $Z = N - 1$ :

$$\begin{aligned} E_a(\text{Ni}) &= 0.0424673, \\ s &= 0.291495. \end{aligned} \quad (\text{D10})$$

The slope was computed from  $E_a(\text{Ni})$  and  $R_{cov}(\text{Ni}) = 2.210980$ .

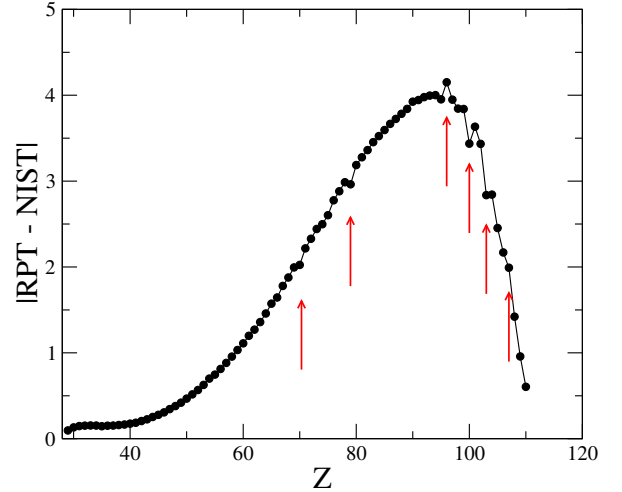


FIG. 21. (Color online) Cu-like systems ( $N = 29$ ). Detected inconsistencies ( $Z = 70$ ,  $79$ ,  $96$ ,  $100$ ,  $103$  and  $107$ ) are marked with red arrows.

#### Discussion:

In the Cu-like sequence (Fig. 21), inconsistencies can be very clearly distinguished. For  $Z = 70$  and  $79$ , data come from Ref. [17]. For  $Z \geq 96$ ,  $I_p$  values are provided by Rodrigues *et al.*<sup>12</sup>. The error bars in these latter cases are greater than the observed deviations.

#### 10. The Zn-like sequence ( $N = 30$ )

RPT coefficients:

$$\begin{aligned} a_2 &= 0.03125 + 0.00634766 (Z/137.0)^2, \\ a_1 &= -1.34713 - 0.0620302 (Z/137.0)^2, \\ a_0 &= 9.2367, \\ a_{-1} &= 131.194. \end{aligned}$$

Conditions at  $Z = N - 1$ :

$$\begin{aligned} E_a(\text{Cu}) &= 0.0453693, \\ s &= 0.285562. \end{aligned} \quad (\text{D11})$$

The slope was computed from  $E_a(\text{Cu})$  and  $R_{cov}(\text{Cu}) = 2.305466$ .

#### Discussion:

In Fig. 22 (the Zn-like sequence), the data for  $Z = 43 - 44$  is taken from the Dirac-Fock calculation of Ref. [12]. On the other hand,  $Z = 45$  ionization potential was collected from the relativistic multireference many-body perturbation theory calculations of Vilkas *et al.*<sup>18</sup>. The  $Z = 74$  ionization potential comes from Ref. [11], as before. For  $Z \geq 96$  the numbers come from [12], with the characteristic large uncertainties.

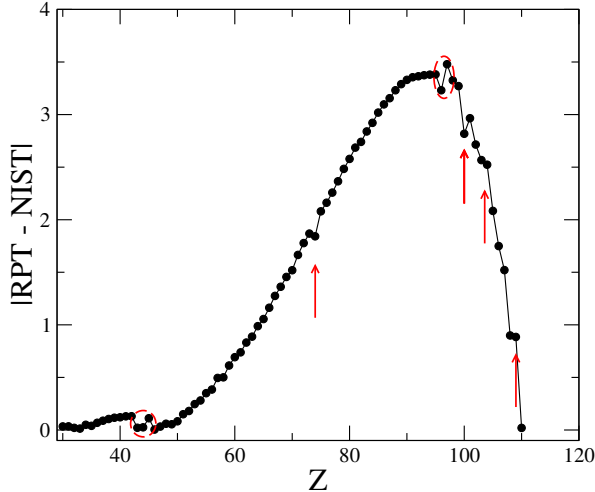


FIG. 22. (Color online) The Zn-like systems ( $N = 30$ ). Detected inconsistencies ( $Z = 43 - 45, 74, 96-97, 100, 104$  and  $109$ ) are marked with red arrows and a discontinuous red ellipse.

### 11. The Ge-like sequence ( $N = 32$ )

RPT coefficients:

$$\begin{aligned} a_2 &= 0.03125 + 0.00634766 (Z/137.0)^2, \\ a_1 &= -1.51951 - 0.0952627 (Z/137.0)^2, \\ a_0 &= 10.9568, \\ a_{-1} &= 185.117. \end{aligned}$$

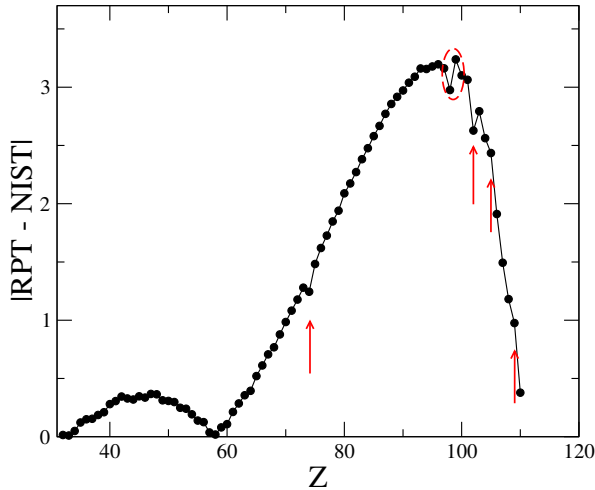


FIG. 23. (Color online) Ge-like ions ( $N = 32$ ). Detected inconsistencies ( $Z = 74, 98-99, 102, 105$  and  $109$ ) are marked with red arrows and a discontinuous red ellipse.

Conditions at  $Z = N - 1$ :

$$\begin{aligned} E_a(\text{Ga}) &= 0.0157966, \\ s &= 0.240629. \end{aligned} \quad (\text{D12})$$

The slope was computed from  $E_a(\text{Ga})$  and  $R_{cov}(\text{Ga}) = 2.324363$ .

### 12. The As-like sequence ( $N = 33$ )

RPT coefficients:

$$\begin{aligned} a_2 &= 0.03125 + 0.00244141 (Z/137.0)^2, \\ a_1 &= -1.55446 - 0.0829917 (Z/137.0)^2, \\ a_0 &= 12.6573, \\ a_{-1} &= 164.459. \end{aligned}$$

Conditions at  $Z = N - 1$ :

$$\begin{aligned} E_a(\text{Ge}) &= 0.0453118, \\ s &= 0.288928. \end{aligned} \quad (\text{D13})$$

The slope was computed from  $E_a(\text{Ge})$  and  $R_{cov}(\text{Ge}) = 2.267671$ .

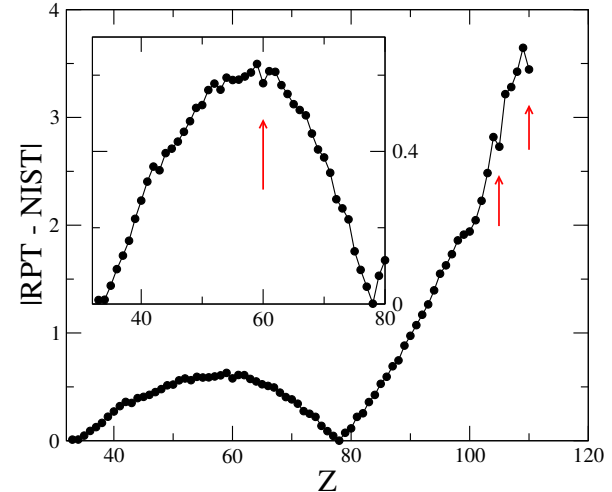


FIG. 24. (Color online) The As-like systems ( $N = 33$ ). Inconsistencies detected at  $Z = 60, 105$  and  $109$  are marked with red arrows.

### Discussion:

In the As-like sequence (Fig. 24) significant deviations are related to the Dirac-Fock calculations of Ref. [12].

### 13. The Se-like sequence ( $N = 34$ )

RPT coefficients:

$$\begin{aligned} a_2 &= 0.03125 + 0.00244141 (Z/137.0)^2, \\ a_1 &= -1.59101 - 0.0853527 (Z/137.0)^2, \\ a_0 &= 11.7569, \\ a_{-1} &= 222.876. \end{aligned}$$

Conditions at  $Z = N - 1$ :

$$E_a(\text{As}) = 0.0295464, \quad s = 0.271227. \quad (\text{D14})$$

The slope was computed from  $E_a(\text{As})$  and  $R_{\text{cov}}(\text{As}) = 2.267671$ .

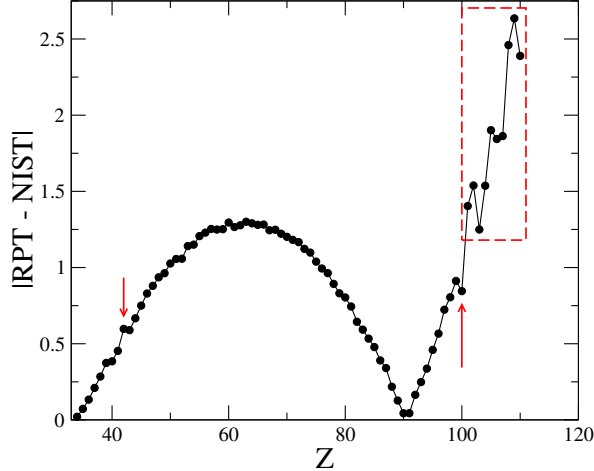


FIG. 25. (Color online) The Se-like sequence ( $N = 34$ ). Detected inconsistencies ( $Z = 42, 100$  and a great dispersion for  $Z \geq 101$ ) are marked with red arrows and a discontinuous red box.

#### Discussion:

In Fig. 25 (Se-like sequence) we detect inconsistencies at  $Z = 42, 100$ , and a great dispersion for  $Z \geq 101$ . Data for  $\text{Mo}^{+18}$  (i.e.  $Z = 42, N = 34$ ) come from Refs. [19] and [20], whereas the ionization potentials for  $Z \geq 100$  are computed in Ref. [12].

#### 14. The Br-like sequence ( $N = 35$ )

RPT coefficients:

$$\begin{aligned} a_2 &= 0.03125 + 0.00244141 (Z/137.0)^2, \\ a_1 &= -1.63074 - 0.0881566 (Z/137.0)^2, \\ a_0 &= 13.0595, \\ a_{-1} &= 215.756. \end{aligned}$$

Conditions at  $Z = N - 1$ :

$$E_a(\text{Se}) = 0.0742704, \quad s = 0.312415. \quad (\text{D15})$$

The slope was computed from  $E_a(\text{Se})$  and  $R_{\text{cov}}(\text{Se}) = 2.229877$ .

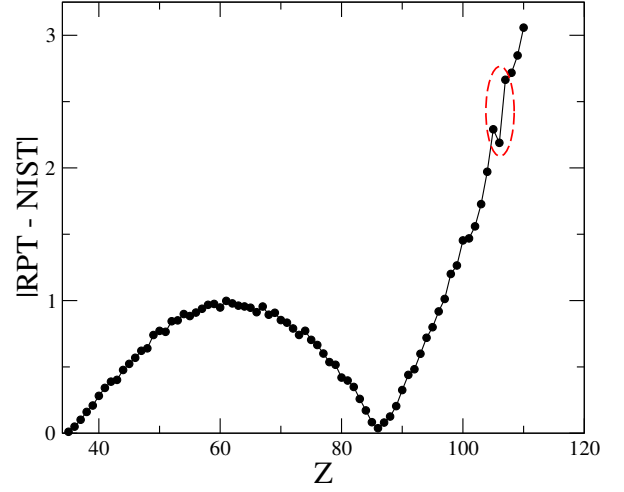


FIG. 26. (Color online) Br-like systems ( $N = 35$ ). A smooth curve. The most significant dispersions occur for  $Z = 105 - 107$ .<sup>12</sup>

#### 15. The Kr-like sequence ( $N = 36$ )

RPT coefficients:

$$\begin{aligned} a_2 &= 0.03125 + 0.00244141 (Z/137.0)^2, \\ a_1 &= -1.66728 - 0.0905176 (Z/137.0)^2, \\ a_0 &= 13.5057, \\ a_{-1} &= 234.611. \end{aligned}$$

Conditions at  $Z = N - 1$ :

$$E_a(\text{Br}) = 0.123625, \quad s = 0.333943. \quad (\text{D16})$$

The slope was computed from  $E_a(\text{Br})$  and  $R_{\text{cov}}(\text{Br}) = 2.210980$ .

#### Appendix E: Fifth row elements

##### 1. The Sr-like sequence ( $N = 38$ )

RPT coefficients:

$$\begin{aligned} a_2 &= 0.03125 + 0.00244141 (Z/137.0)^2, \\ a_1 &= -1.86543 - 0.136324 (Z/137.0)^2, \\ a_0 &= 15.882, \\ a_{-1} &= 388.488. \end{aligned}$$

Conditions at  $Z = N - 1$ :

$$E_a(\text{Rb}) = 0.0178511, \quad s = 0.166529. \quad (\text{E1})$$

The slope was computed from  $E_a(\text{Rb})$  and  $R_{\text{cov}}(\text{Rb}) = 4.062911$ .

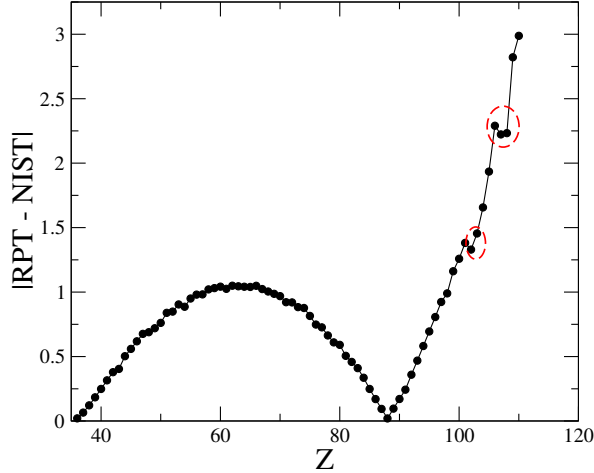


FIG. 27. (Color online) The Kr-like systems ( $N = 36$ ). Detected inconsistencies ( $Z = 102$ - $103$ , and  $106$ - $108$ ) are marked with discontinuous red ellipses.

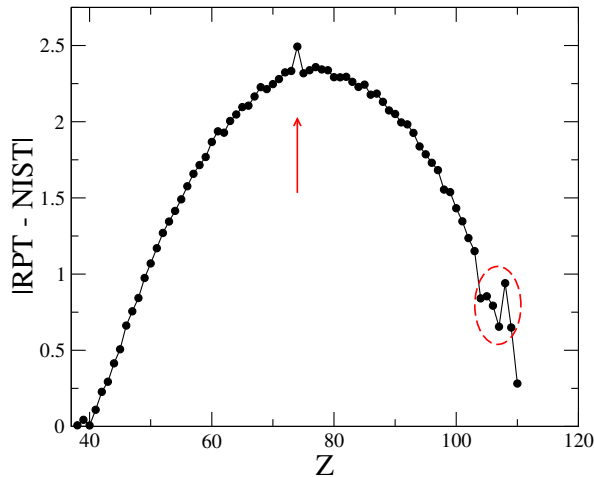


FIG. 28. (Color online) The Sr-like systems ( $N = 38$ ). Detected inconsistencies ( $Z = 74$   $^{11}$  and  $104$ - $109$   $^{12}$ ) are marked with a red arrow and a discontinuous red ellipse.

## 2. The Y-like sequence ( $N = 39$ )

RPT coefficients:

$$\begin{aligned} a_2 &= 0.03125 + 0.00244141 (Z/137.0)^2, \\ a_1 &= -1.94905 - 0.142908 (Z/137.0)^2, \\ a_0 &= 16.4347, \\ a_{-1} &= 476.155. \end{aligned}$$

$$a_{-1} = 504.63.$$

Conditions at  $Z = N - 1$ :

$$\begin{aligned} E_a(\text{Sr}) &= 0.00176347, \\ s &= 0.120083. \end{aligned} \tag{E2}$$

The slope was computed from  $E_a(\text{Sr})$  and  $R_{cov}(\text{Sr}) = 3.590480$ .

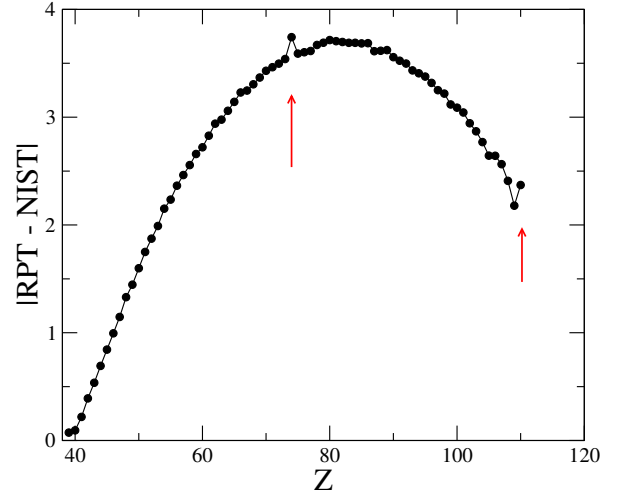


FIG. 29. (Color online) The Y-like systems ( $N = 39$ ). Detected inconsistencies ( $Z = 74$   $^{11}$  and  $110$   $^{12}$ ) are marked with red arrows.

## 3. The Zr-like sequence ( $N = 40$ )

RPT coefficients:

$$\begin{aligned} a_2 &= 0.03125 + 0.00244141 (Z/137.0)^2, \\ a_1 &= -1.94905 - 0.142908 (Z/137.0)^2, \\ a_0 &= 16.4347, \\ a_{-1} &= 476.155. \end{aligned}$$

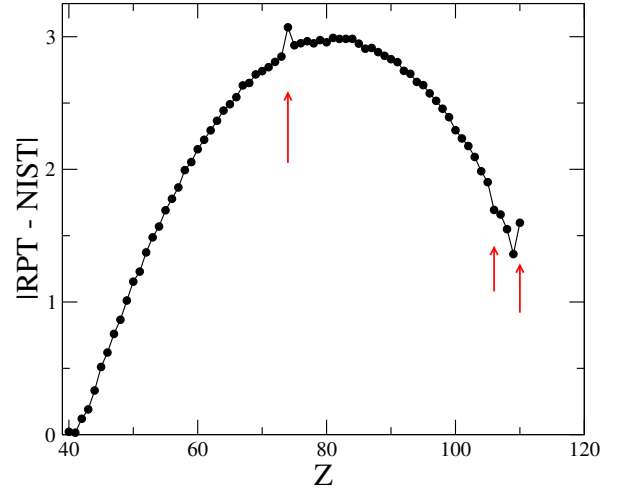


FIG. 30. (Color online) The Zr-like sequence ( $N = 40$ ). Detected inconsistencies ( $Z = 74$ ,  $^{11}$   $106$  and  $110$   $^{12}$ ) are marked with red arrows.

Conditions at  $Z = N - 1$ :

$$\begin{aligned} E_a(\text{Y}) &= 0.0112782, \\ s &= 0.179247. \end{aligned} \tag{E3}$$

The slope was computed from  $E_a(Y)$  and  $R_{cov}(Y) = 3.325918$ .

#### 4. The Nb-like sequence ( $N = 41$ )

RPT coefficients:

$$\begin{aligned} a_2 &= 0.03125 + 0.00113932 (Z/137.0)^2, \\ a_1 &= -1.99199 - 0.112623 (Z/137.0)^2, \\ a_0 &= 17.6019, \\ a_{-1} &= 492.881. \end{aligned}$$

Conditions at  $Z = N - 1$ :

$$\begin{aligned} E_a(\text{Zr}) &= 0.0156496, \\ s &= 0.198128. \end{aligned} \quad (\text{E4})$$

The slope was computed from  $E_a(\text{Zr})$  and  $R_{cov}(\text{Zr}) = 3.099151$ .

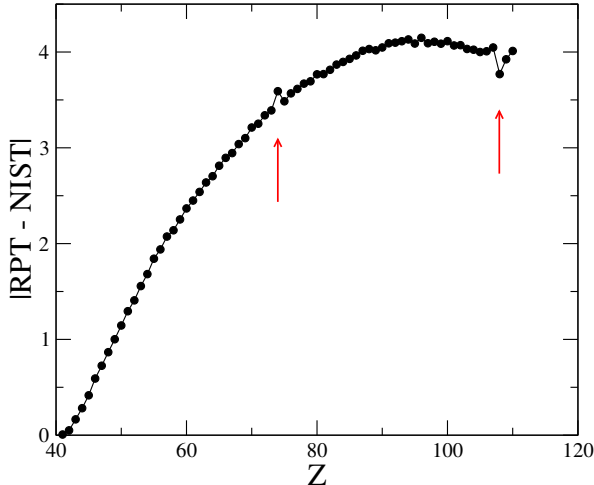


FIG. 31. (Color online) The Nb-like systems ( $N = 41$ ). Detected inconsistencies ( $Z = 74^{11}$  and  $108^{12}$ ) are marked with red arrows.

#### 5. The Mo-like sequence ( $N = 42$ )

RPT coefficients:

$$\begin{aligned} a_2 &= 0.03125 + 0.00113932 (Z/137.0)^2, \\ a_1 &= -2.03196 - 0.114317 (Z/137.0)^2, \\ a_0 &= 18.7868, \\ a_{-1} &= 503.25. \end{aligned}$$

Conditions at  $Z = N - 1$ :

$$\begin{aligned} E_a(\text{Nb}) &= 0.0336625, \\ s &= 0.229290. \end{aligned} \quad (\text{E5})$$

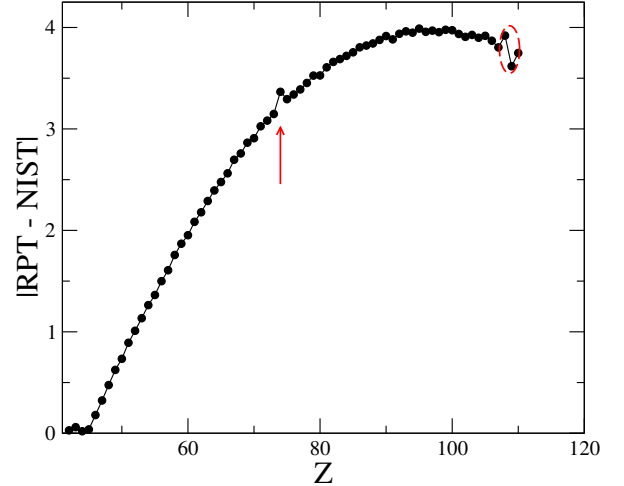


FIG. 32. (Color online) The Mo-like ions ( $N = 42$ ). Detected inconsistencies ( $Z = 74^{11}$  and  $108^{12}$ ) are marked with a red arrow and a discontinuous red ellipse.

The slope was computed from  $E_a(\text{Nb})$  and  $R_{cov}(\text{Nb}) = 2.947973$ .

#### 6. The Tc-like sequence ( $N = 43$ )

RPT coefficients:

$$\begin{aligned} a_2 &= 0.03125 + 0.00113932 (Z/137.0)^2, \\ a_1 &= -2.07354 - 0.116109 (Z/137.0)^2, \\ a_0 &= 19.0013, \\ a_{-1} &= 556.886. \end{aligned}$$

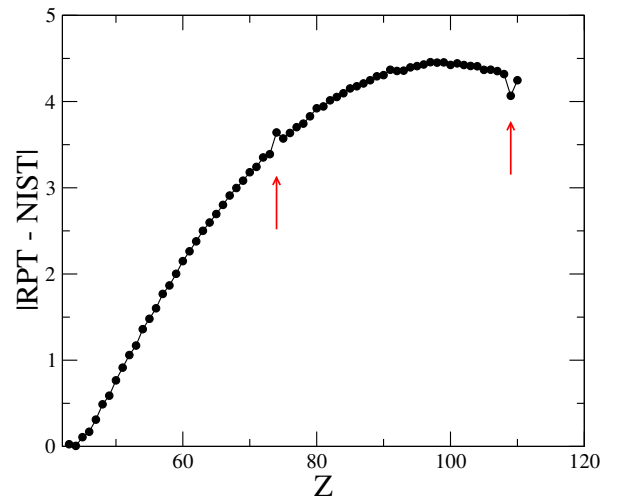


FIG. 33. (Color online) The Tc-like ions ( $N = 43$ ). Detected inconsistencies ( $Z = 74^{11}$  and  $109^{12}$ ) are marked with red arrows.

Conditions at  $Z = N - 1$ :

$$E_a(\text{Mo}) = 0.0274790, \\ s = 0.233850. \quad (\text{E6})$$

The slope was computed from  $E_a(\text{Mo})$  and  $R_{cov}(\text{Mo}) = 2.759000$ .

### 7. The Ru-like sequence ( $N = 44$ )

RPT coefficients:

$$a_2 = 0.03125 + 0.00113932 (Z/137.0)^2, \\ a_1 = -2.11747 - 0.118053 (Z/137.0)^2, \\ a_0 = 19.1396, \\ a_{-1} = 621.055.$$

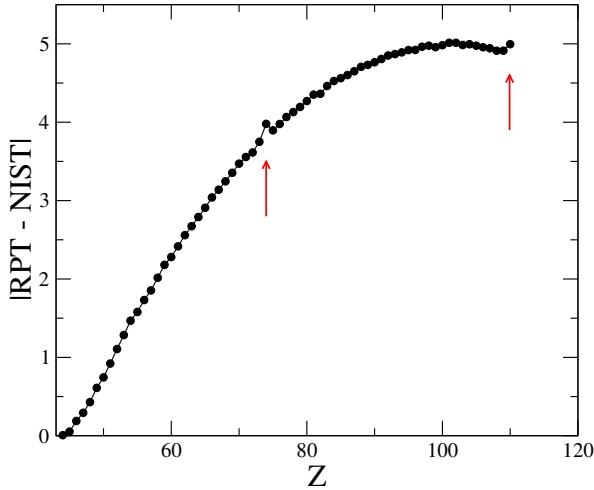


FIG. 34. (Color online) The Ru-like systems ( $N = 44$ ). Detected inconsistencies ( $Z = 74$  and  $110$ ) are marked with red arrows.

Conditions at  $Z = N - 1$ :

$$E_a(\text{Tc}) = 0.0202049, \\ s = 0.232165. \quad (\text{E7})$$

The slope was computed from  $E_a(\text{Tc})$  and  $R_{cov}(\text{Tc}) = 2.607822$ .

### 8. The Rh-like sequence ( $N = 45$ )

RPT coefficients:

$$a_2 = 0.03125 + 0.00113932 (Z/137.0)^2, \\ a_1 = -2.15904 - 0.119845 (Z/137.0)^2, \\ a_0 = 20.2974, \\ a_{-1} = 640.445.$$

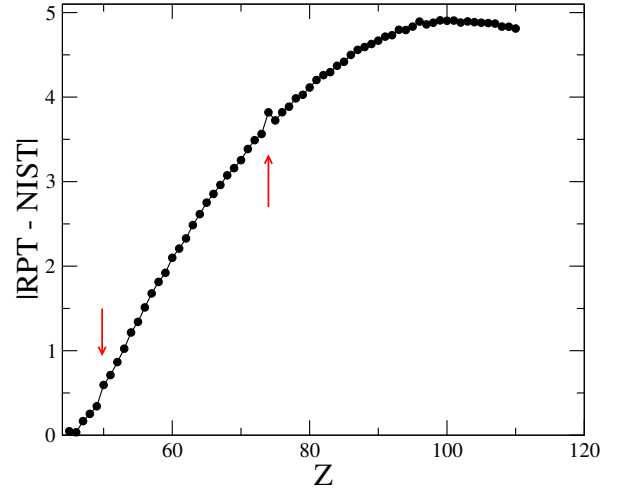


FIG. 35. (Color online) Rh-like systems ( $N = 45$ ). Detected inconsistencies (The jump at  $Z = 50$ <sup>12</sup> and the deviation at  $Z = 74$ <sup>11</sup>) are marked with red arrows.

Conditions at  $Z = N - 1$ :

$$E_a(\text{Ru}) = 0.0385732, \\ s = 0.232165. \quad (\text{E8})$$

The slope was computed from  $E_a(\text{Ru})$  and  $R_{cov}(\text{Ru}) = 2.570028$ .

### 9. The Pd-like sequence ( $N = 46$ )

RPT coefficients:

$$a_2 = 0.03125 + 0.00113932 (Z/137.0)^2, \\ a_1 = -2.19902 - 0.121538 (Z/137.0)^2, \\ a_0 = 20.4131, \\ a_{-1} = 703.998.$$

Conditions at  $Z = N - 1$ :

$$E_a(\text{Rh}) = 0.0417692, \\ s = 0.258127. \quad (\text{E9})$$

The slope was computed from  $E_a(\text{Rh})$  and  $R_{cov}(\text{Rh}) = 2.532233$ .

#### Discussion:

In the Pd-like sequence (Fig. 36), in addition to  $Z = 74$ , an apparent inconsistency at  $Z = 55$  comes from the experimental work of Churilov *et al.*<sup>21</sup>

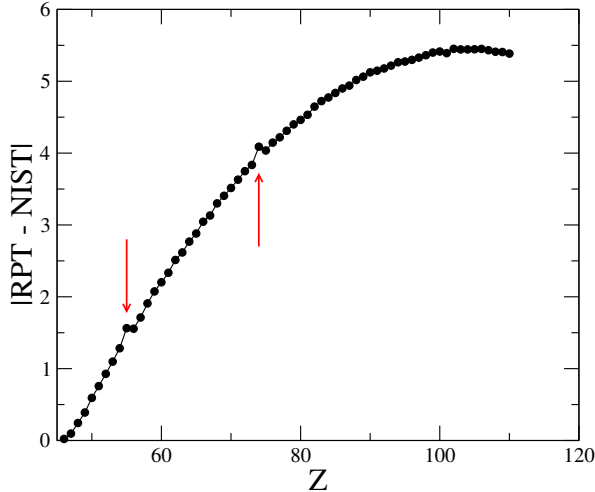


FIG. 36. (Color online) The Pd-like sequence ( $N = 46$ ). Detected inconsistencies ( $Z = 55$  and  $74$ ) are marked with red arrows.

#### 10. The Ag-like sequence ( $N = 47$ )

RPT coefficients:

$$\begin{aligned} a_2 &= 0.03125 + 0.00113932 (Z/137.0)^2, \\ a_1 &= -2.41502 - 0.161518 (Z/137.0)^2, \\ a_0 &= 35.8484, \\ a_{-1} &= 446.393. \end{aligned}$$

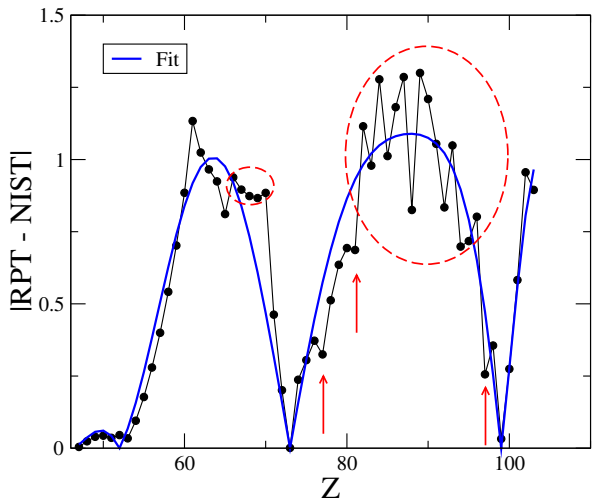


FIG. 37. (Color online) The Ag-like systems ( $N = 47$ ). Detected inconsistencies ( $66 \leq Z \leq 70$ ,  $Z = 77$ ,  $81$ ,  $97$ , and the great dispersion of points for  $82 \leq Z \leq 96$ ) are marked with red arrows and discontinuous red ellipses.

Conditions at  $Z = N - 1$ :

$$\begin{aligned} E_a(\text{Pd}) &= 0.0206460, \\ s &= 0.263779. \end{aligned} \quad (\text{E10})$$

The slope was computed from  $E_a(\text{Pd})$  and  $R_{\text{cov}}(\text{Pd}) = 2.456644$ .

#### Discussion:

A qualitatively different picture appears in the Ag-like sequence, Fig. 37. The maximum of  $|\text{RPT} - \text{NIST}|$  diminished, as compared with the Pd-like sequence, but the dispersion of points has significantly increased. Problematic points in the interval  $66 \leq Z \leq 70$  come from Ref. [12], whereas data for  $Z \geq 77$  is the entire responsibility of Carlson *et al.*<sup>22</sup>, who employ a simple spherical shell model in order to compute the ionization potentials. Deviations are, however, within indicated error bars. As a reference, we use a fit by means of Eq. (D2) with three interior crossing points (blue curve).

#### 11. The Cd-like sequence ( $N = 48$ )

RPT coefficients:

$$\begin{aligned} a_2 &= 0.03125 + 0.00113932 (Z/137.0)^2, \\ a_1 &= -2.46174 - 0.163993 (Z/137.0)^2, \\ a_0 &= 37.7704, \\ a_{-1} &= 449.257. \end{aligned}$$

Conditions at  $Z = N - 1$ :

$$\begin{aligned} E_a(\text{Ag}) &= 0.0478309, \\ s &= 0.265692. \end{aligned} \quad (\text{E11})$$

The slope was computed from  $E_a(\text{Ag})$  and  $R_{\text{cov}}(\text{Ag}) = 2.570028$ .

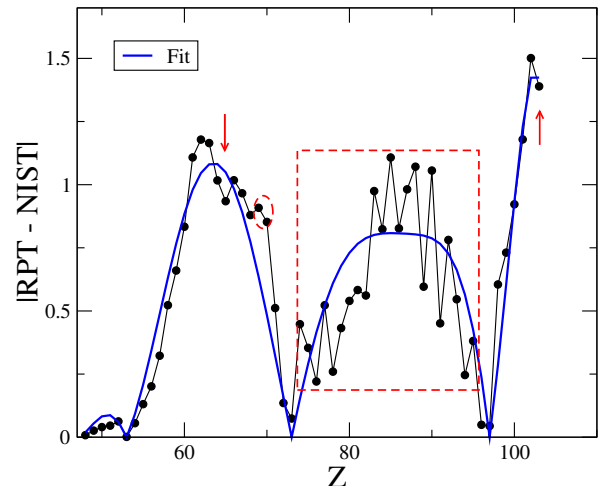


FIG. 38. (Color online) The Cd-like systems ( $N = 48$ ). Detected inconsistencies ( $Z = 65$ ,  $69$ - $70$ ,  $103$  and the dispersion of points for  $74 \leq Z \leq 95$ ) are marked with red arrows, ellipse and box.

### Discussion:

In the Cd-like ions (Fig. 38), Ref. [22] provides most of the data for  $61 \leq Z \leq 97$ , with the only exceptions of  $Z = 61$ , coming from Ref. [12], and  $Z = 74$  from Ref. [11]. We shall stress the large relative error bars indicated for  $Z \geq 72$ .

### 12. The Sn-like sequence ( $N = 50$ )

RPT coefficients:

$$\begin{aligned} a_2 &= 0.03125 + 0.00113932 (Z/137.0)^2, \\ a_1 &= -2.56241 - 0.169401 (Z/137.0)^2, \\ a_0 &= 37.191, \\ a_{-1} &= 688.884. \end{aligned}$$

Conditions at  $Z = N - 1$ :

$$\begin{aligned} E_a(\text{In}) &= 0.0110208, \\ s &= 0.205786. \end{aligned} \quad (\text{E12})$$

The slope was computed from  $E_a(\text{In})$  and  $R_{cov}(\text{In}) = 2.683411$ .

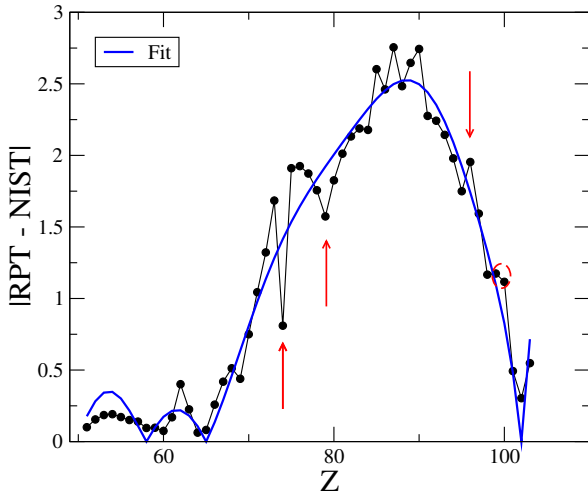


FIG. 39. (Color online) The Sn-like systems ( $N = 50$ ). Detected inconsistencies ( $Z = 74,^{11} 79, 96$ , and  $99 - 100^{22}$ ) are marked with red arrows.

### 13. The Sb-like sequence ( $N = 51$ )

RPT coefficients:

$$\begin{aligned} a_2 &= 0.03125 + 0.00113932 (Z/137.0)^2, \\ a_1 &= -2.61122 - 0.172008 (Z/137.0)^2, \\ a_0 &= 40.6766, \\ a_{-1} &= 628.32. \end{aligned}$$

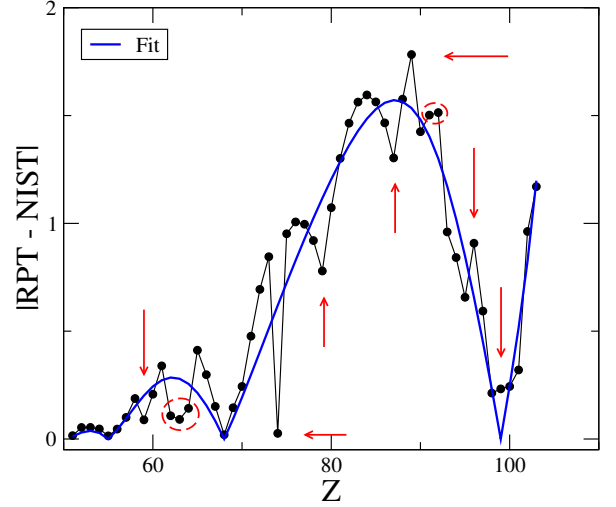


FIG. 40. (Color online) The Sb-like sequence ( $N = 51$ ). Detected inconsistencies ( $Z = 74,^{11} 59, 62-64, 79, 87, 91-92$ , 96 and  $99^{22}$ ) are marked with red arrows.

Conditions at  $Z = N - 1$ :

$$\begin{aligned} E_a(\text{Sn}) &= 0.0408532, \\ s &= 0.254716. \end{aligned} \quad (\text{E13})$$

The slope was computed from  $E_a(\text{Sn})$  and  $R_{cov}(\text{Sn}) = 2.645617$ .

### 14. The Te-like sequence ( $N = 52$ )

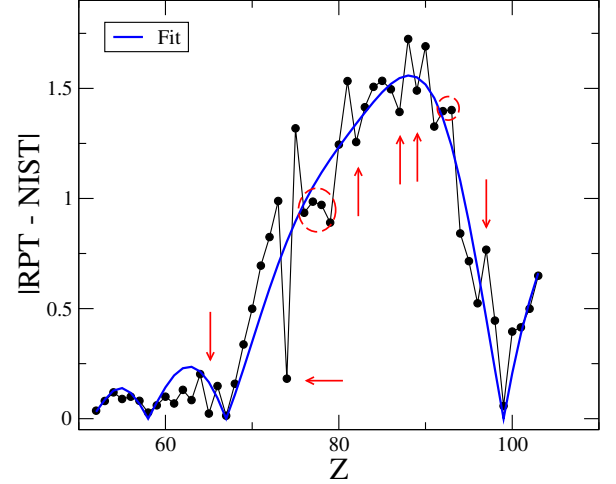


FIG. 41. (Color online) The Te-like systems ( $N = 52$ ). Detected inconsistencies ( $Z = 74,^{11} 65, 76-79, 82, 87, 89$ , 92-93, and  $97^{22}$ ) are marked with red arrows and ellipse.

RPT coefficients:

$$\begin{aligned} a_2 &= 0.03125 + 0.00113932 (Z/137.0)^2, \\ a_1 &= -2.65793 - 0.174483 (Z/137.0)^2, \\ a_0 &= 41.4216, \\ a_{-1} &= 699.342. \end{aligned}$$

Conditions at  $Z = N - 1$ :

$$\begin{aligned} E_a(\text{Sb}) &= 0.0384262, \\ s &= 0.252618. \end{aligned} \quad (\text{E14})$$

The slope was computed from  $E_a(\text{Sb})$  and  $R_{\text{cov}}(\text{Sb}) = 2.645617$ .

### 15. The I-like sequence ( $N = 53$ )

RPT coefficients:

$$\begin{aligned} a_2 &= 0.03125 + 0.000488281 (Z/137.0)^2, \\ a_1 &= -2.71192 - 0.133452 (Z/137.0)^2, \\ a_0 &= 44.5066, \\ a_{-1} &= 670.563. \end{aligned}$$

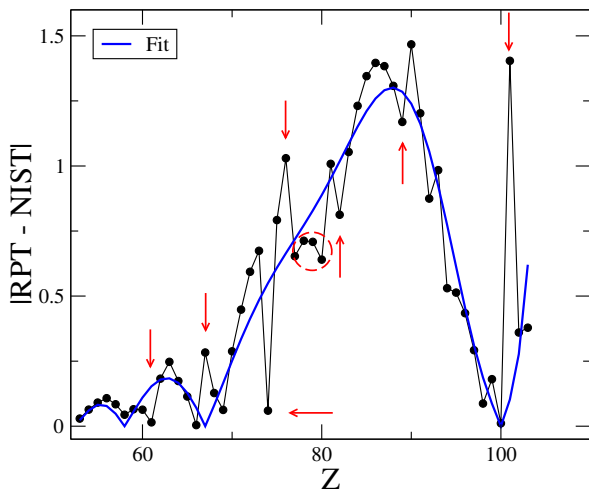


FIG. 42. (Color online) The case of I-like systems ( $N = 53$ ). Detected inconsistencies ( $Z = 74,^{11} 61, 67, 76, 77-80, 82, 89$ , and  $101^{22}$ ) are marked with red arrows and ellipse.

Conditions at  $Z = N - 1$ :

$$\begin{aligned} E_a(\text{Te}) &= 0.0724331, \\ s &= 0.278176. \end{aligned} \quad (\text{E15})$$

The slope was computed from  $E_a(\text{Te})$  and  $R_{\text{cov}}(\text{Te}) = 2.588925$ .

### 16. The Xe-like sequence ( $N = 54$ )

RPT coefficients:

$$\begin{aligned} a_2 &= 0.03125 + 0.000488281 (Z/137.0)^2, \\ a_1 &= -2.75916 - 0.134776 (Z/137.0)^2, \\ a_0 &= 46.3287, \\ a_{-1} &= 694.4. \end{aligned}$$

Conditions at  $Z = N - 1$ :

$$\begin{aligned} E_a(\text{I}) &= 0.112416, \\ s &= 0.293706. \end{aligned} \quad (\text{E16})$$

The slope was computed from  $E_a(\text{I})$  and  $R_{\text{cov}}(\text{I}) = 2.570028$ .

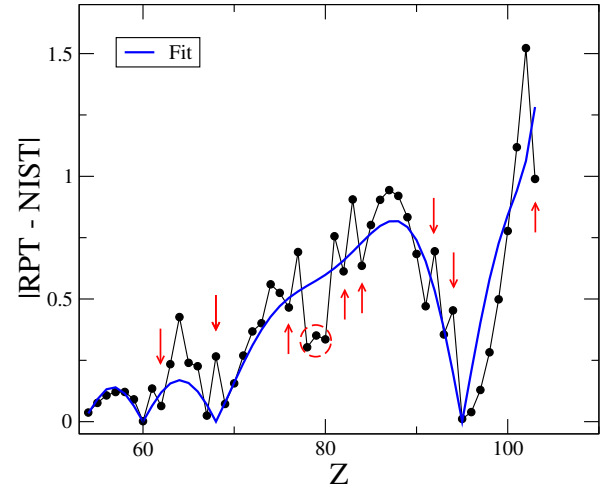


FIG. 43. (Color online) The Xe-like systems ( $N = 54$ ). Detected inconsistencies ( $Z = 62, 68, 76, 78-80, 82, 84, 92, 94$  and  $103^{22}$ ) are marked with red arrows and a discontinuous red ellipse.

- 
- [1] R. Carcassés, A. González, Phys. Rev. A 80, 024502 (2009).  
[2] A. Kramida, Yu. Ralchenko, J. Reader, and NIST ASD Team (2012). NIST Atomic Spectra Database (ver. 5.0), [Online]. Available: <http://physics.nist.gov/asd> [2013, March 4]. National Institute of Standards and Technol-

- ogy, Gaithersburg, MD.  
[3] C.J. Sansonetti, G. Nave, J. Reader, F. Kerber, The Astrophysical Journal Supplement Series, 202, 15 (2012).  
[4] G. Gil and A. González, eprint arXiv:1309.4392v1 [physich.atom-ph] (2013).  
[5] A. Matulis and F.M. Peeters, J. Phys.: Cond. Matter 6,

- 7751 (1994).
- [6] A. González, A. Pérez, *Int. J. Mod. Phys. B* 12, 2129 (1998).
- [7] A. González, B. Partoens, A. Matulis, F.M. Peeters, *Phys. Rev. B* 59 (3), 1653 (1998).
- [8] A. González, I. Mikhailov, *Int. J. Mod. Phys. B* 11, 3469 (1997).
- [9] G. Gil, A. González, *Mod. Phys. Lett. B* 27, 1350178 (2013).
- [10] Royal Society of Chemistry website <http://www.rsc.org/periodic-table/>. Data References: W.M. Haynes (ed.) CRC Handbook of Chemistry and Physics, CRC Press, Boca Raton, 2011; G.W.C. Kaye and T.H. Laby, Tables of Physical and Chemical Constants, Longman, Essex, 1995.
- [11] A.E. Kramida, J. Reader, *At. Data Nucl. Data Tables* 92, 457479 (2006).
- [12] G.C. Rodrigues, P. Indelicato, J.P. Santos, P. Patt, F. Parente, *At. Data Nucl. Data Tables* 86, 117233 (2004).
- [13] A.N. Artemyev, V.M. Shabaev, V.A. Yerokhin, G. Plunien, and G. Soff, *Phys. Rev. A* 71, 062104 (2005).
- [14] E. Biémont, Y. Frémat, P. Quinet, *At. Data Nucl. Data Tables* 71, 117146 (1999).
- [15] J. Sugar, C. Corliss, *J. Phys. Chem. Ref. Data* 14, Suppl. 2, 1664 (1985).
- [16] J. Sugar and A. Musgrove, *J. Phys. Chem. Ref. Data* 22, 12131278 (1993).
- [17] N. Tragin, J.-P. Geindre, C. Chenais-Popovics, J.-C. Gauthier, J.-F. Wyart, E. Luc-Koenig, *Phys. Rev. A* 39, 20852089 (1989).
- [18] M.J. Vilkas, Y. Ishikawa, K. Hirao, *Chem. Phys. Lett.* 321, 243-252 (2000).
- [19] S. Khatoon, M. S. Z. Chaghtai, and K. Rahimullah, *Phys. Scr.* 19, 2224 (1979).
- [20] J. Sugar and A. Musgrove, *J. Phys. Chem. Ref. Data* 17, 155239 (1988).
- [21] S.S. Churilov, Y.N. Joshi, and A.N. Ryabtsev, *J. Phys. B* 27, 54855495 (1994).
- [22] T.A. Carlson, C.W. Nestor Jr., N. Wasserman, J.D. McDowell, *At. Data Nucl. Data Tables* 2, 63 (1970).